Pattern Recognition Letters 108 (2018) 23–30

Contents lists available at ScienceDirect

Pattern Recognition Letters

journal homepage: www.elsevier.com/locate/patrec

Local directional ZigZag pattern: A rotation invariant descriptor for texture classification

Swalpa Kumar Roy[a,*], Bhabatosh Chanda[a], Bidyut B. Chaudhuri[b], Soumitro Banerjee[c], Dipak Kumar Ghosh[d], Shiv Ram Dubey[e]

[a] Electronics & Communication Sciences Unit, Indian Statistical Institute, Kolkata, India
[b] Computer Vision & Pattern Recognition Unit, Indian Statistical Institute, Kolkata, India
[c] Department of Physical Sciences, Indian Institute of Science Education and Research, Mohanpur Campus, Kolkata, India
[d] Electronics & Communication Engineering, Adamas University, West Bengal, India
[e] Department of Computer Science & Engineering, Indian Institute of Information Technology, Sri City, Chittoor, India

ARTICLE INFO

Article history:
Received 13 June 2017
Available online 1 March 2018

Keywords:
Local ZigZag Pattern (LZP)
Local Directional ZigZag Pattern (LDZP)
Rotation invariance
Texture classification

ABSTRACT

Local feature descriptors play a key role in texture classification tasks. However, such traditional descriptors are deficient to capture the edges and orientations information and local intrinsic structure of images. This letter introduces a simple, new, yet powerful rotation invariant texture descriptor named Local Directional ZigZag Pattern (LDZP) by ZigZag scanning for effective representation of texture. Here at first we compute the directional edge information, so called local directional edge map (LDEM) of a texture image using the Kirsch compass mask in six different directions. Then Local ZigZag Pattern (LZP) is extracted from all LDEM images. Basically, the LZP characterizes the spatial ZigZag structure based on the relation between reference pixel and its adjacent neighboring pixels and is insensitive to the illumination changes. Finally, the uniform pattern histograms are computed from all directional LZP maps which are concatenated to form the final LDZP descriptor. Extensive experiments on texture classification shows the proposed LDZP descriptor achieves state-of-the-art performance in terms of average classification accuracy when applied to the large and well-known benchmark Outex database. We have also shown that LDZP descriptor is equally powerful for human face recognition.

1. Introduction

Texture is ubiquitous in natural images that carries fundamental characteristic of appearance of all natural surfaces. Texture classification is one of the active and challenging problems in texture analysis. It has drawn a lot of attention during the past decades as it plays a crucial role in the area of pattern recognition and computer vision. It has a wide range of applications such as medical image analysis, remote sensing, fabric inspection, segmentation and content-based image retrieval [1], it also includes iris based biometric recognition. Since feature extraction is often performed locally based on regions of the neighborhood, most research efforts have been directed to various local neighborhood patterns of an image. An important issue is how to represent the texture effectively. Basically, texture representation can be categorized in terms of the employed approaches, i.e. geometrical, structural, model-based, statistical, and signal processing. Earlier texture classification methods focus on the statistical analysis of texture images which include the co-occurrence matrix based approach [2] and filtering based techniques [3]. These methods provide good classification performance as long as both training and test sample images have identical orientations. However, arbitrary rotations which could occur in a real-world scene, affect the performance of statistical methods. Therefore, rotation invariance is a crucial issue to be addressed and attention has been focused on the design of geometrically and photometrically invariant local texture representation [4–9]. This paper concentrated on the problem of rotation invariant texture representation.

The extraction of rotation invariant features is usually a complex process where spacial care is required in intermediate step which is computationally demanding [10]. The literature of computer vision shows the work on this aspect has started in the nineties of last century [11]. Kashyap and Khotanzad first proposed circular autoregressive dense approach [12] for the rotation invariance texture classification. Many models have been explored for rotation invariance texture classification, including multi-resolution [13], hidden Markov model [14], and Gaussian Markov model [15].

* Corresponding author.
E-mail address: swalpa@students.iiests.ac.in (S.K. Roy).

https://doi.org/10.1016/j.patrec.2018.02.027
0167-8655/

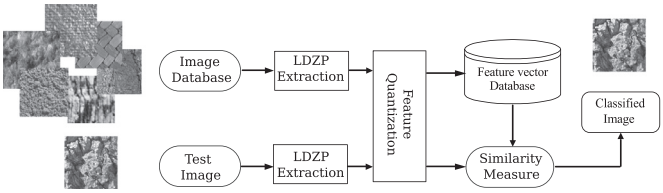

Fig. 1. Proposed texture classification framework.

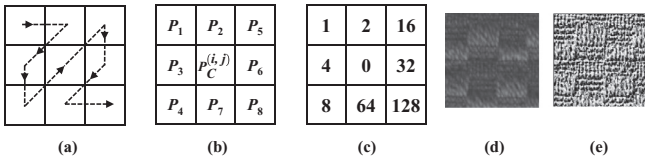

Fig. 2. (a) Local ZigZag structure of a patch. (b) Patch pixel representation based on ZigZag structure. (c) Weights of the local ZigZag pattern of the patch. (d) Original texture sample. (e) LZP pattern of the texture sample.

Recently Varma and Zisserman proposed VZ-MR8 [5] to learn a texton dictionary from a set of training images which are rotation and scale invariant and then classified the unknown sample images using learned texton distributions. Later, Varma and Zisserman proposed VZ-Patch [7], another texton based algorithm to represent the feature distribution, which extracts texton from local image intensity directly. The downside of these methods are feature extraction and matching times which is not very favourable.

In 1996 a simple and computationally efficient texture representation, called local binary pattern (LBP) was proposed by Ojala et al. [16], which is invariant to the uniform intensity changes. The LBP has been widely used in other domains such as texture segmentation, face recognition, shape localization and object recognition [17]. Variants of LBP have been proposed due to immense success of LBP in pattern recognition and computer vision problems. Liaor et al. [18] proposed DLBP, a dominant pattern by encoding only the most frequently occurred patterns (around 80%) to improve the performance. Guo et al. introduced LBP variance (LBPV) [19] and completed LBP (CLBP) [20] to enhance the descriptive power and improve the texture classification, for effective recognition of face images, Zhang et al. [21] used local derivative pattern (LDP) with higher order and showed that LDP performs much better than conventional LBP. Dubey et al. introduced LWP [22] to find the histogram feature vector for biomedical image retrieval. Guo et al. introduced a local directional derivative pattern (LDDP) [23] which includes the directional information with LDP for rotation invariant texture classification. Tan and Triggs introduced local ternary pattern (LTP) [24] and Liu et al. proposed [25] noise tolerant descriptor to improve the texture classification performance under varying illumination and noisy conditions. Mehta and Egazarian proposed a variant of LBP so-called DRLBP descriptor for rotation invariant texture classification. Recently, Roy et al. [26] introduced a complete dual-cross pattern (CDCP) to address the scale and rotational effects in unconstrained texture classification.

However, most of the descriptors are based on the same basic idea of LBP and extracts only circular isotropic micro structure of the texture image which is not enough to describe the texture information and do not sufficiently address the rotation invariant issues. Hence, inspired by the ZigZag scanning of discrete cosine transform (DCT) [27] coding technique, a new image descriptor called Local Directional ZigZag Pattern (LDZP) is proposed for effective texture representation and classification. The readers should not confuse the ZigZag scanning of DCT encoding which perform in frequency domain for data compression, with our ZigZag scanning of LDZP, performed in spatial domain to select the ordering for generating the descriptor. The schematic diagram of proposed LDZP based texture classification framework is shown in Fig. 1.

The main contributions of this letter are as follows: We propose a Local ZigZag Pattern (LZP) where sampling points fall exactly at the integer pixel position and avoids inaccuracy of interpolation of gray values, characterizes the spatial local ZigZag structure of a texture image; The LZP presents a strong angular relation between two consecutive pixels with respect to the center as well as two alternate pixels with respect to their intermediate pixel which makes it more efficient to capture non-uniform local texture pattern; To compute the LDZP descriptor we calculate local directional edge map (LDEM) of a texture image using the Kirsch compass mask in six different directions and encode all directional edge responses using LZP which reduces the noise effects; The uniform pattern histograms are computed from all directional LZP maps to reduce the dimension. Finally all the histograms are concatenated to create the LDZP descriptor, which encodes the directional LZP pattern information and makes the descriptor invariance to rotation.

The rest of the letter is organized as follows. Section 2 describes the details of proposed local ZigZag pattern (LZP). The proposed local directional ZigZag pattern (LDZP) descriptor is presented in Section 3. The effectiveness of the LZP over LBP are discussed in Section 4. Section 5 describes the evaluation criteria. The experimental results are summarized in Section 6 and the conclusion is drawn in Section 7.

2. Local ZigZag pattern

This work introduces a novel and efficient texture descriptor from the relation between a center pixel and its local neighboring pixels by ZigZag scanning, called local ZigZag pattern (LZP). Hence LZP is a local gray scale texture descriptor which represents the local spatial ZigZag structure of a texture image as shown in Fig. 2(a). Let in a gray-scale image I, $P_c^{(i,j)}$ be the center pixel of a 3×3 local neighboring window having gray value $I_c^{i,j}$ and the nth neighbors of $P_c^{(i,j)}$ are denoted by $P_n^{(i,j)}$ around the center pixel $P_c^{(i,j)}$ having gray value $I_n^{(i,j)}$ in a ZigZag fashion as depicted in Fig. 2(b), where n is a positive integer and $n \in [1, N]$. The value of N (number of neighbors) in Fig. 2(b) is 8. The local texture of the monochrome image I is represented by the joint distribution of gray value difference between the center pixel and its N neighbors ($N > 0$) defined as follows,

$$T^{(i,j)} = \tau(I_1^{(i,j)} - I_c^{(i,j)}, I_2^{(i,j)} - I_c^{(i,j)}, \ldots, I_N^{(i,j)} - I_c^{(i,j)})$$

where (τ) represents the joint distribution function. In order to encode the texture information using local ZigZag pattern, we consider only the signs of the differences $sign(I_n^{(i,j)} - I_c^{(i,j)})$ which make LZP invariant under monotonic photometric changes, hence the operator LZP is robust to lighting effects and is defined as,

$$\text{LZP}(i, j) = \sum_{n=1}^{N} sign(I_n^{(i,j)} - I_c^{(i,j)}) \times 2^{n-1}, \quad (1)$$

$$sign(z) = \begin{cases} 1, & if\ z \geq 0 \\ 0, & else. \end{cases}$$

The sign of differences between center and its neighborhoods is described as a N-bit binary string, where 2^{n-1} represents the weight value of nth bit (Fig. 2(c)), resulting in 2^N distinct decimal values for the LZP code. Since we are dealing with 3×3 local neighboring window, the value of LZP code for each pixel is in the range between 0 and 255. Fig. 2(a)–(e) shows the local ZigZag structure of a patch, patch pixel representation based on ZigZag structure, weights of the local ZigZag pattern of the patch, a original texture sample and LZP pattern of the texture sample, respectively. After extracting the LZP pattern for each pixel (x, y) of the

texture image of sizes $M_x \times M_y$, the distribution of local gray scale i.e. texture pattern is represented by building a 2^N bins discrete distribution of LZP codes, given by

$$H(\lambda) = \sum_{i=2}^{M_x-1} \sum_{j=2}^{M_y-1} f(\text{LZP}_N(i,j), \lambda), \lambda \in [0, L] \tag{2}$$

$$f(u,v) = \begin{cases} 1, & u == v \\ 0, & else \end{cases}$$

where L is the maximal value of LZP pattern. The LZP descriptor is further extended to *uniform* pattern, where a uniformity measure, U encodes the number of bitwise 1/0 transition (spatial changes) in a N-bit pattern, defined as,

$$\begin{aligned} U(\text{LZP}_N) =& \mid s(I_N^{i,j} - I_c^{i,j}) - s(I_1^{i,j} - I_c^{i,j}) \mid \\ &+ \sum_{n=2}^{N} \mid s(I_n^{i,j} - I_c^{i,j}) - s(I_{n-1}^{i,j} - I_c^{i,j}) \mid \end{aligned} \tag{3}$$

For example, the U values of LZP strings 11111111 and 00000010 are 0 and 2, respectively. The *uniform* LZP pattern refers to the uniform appearance of string which has restricted transitions ($U \leq 2$) in the N-bit circular binary strings [4]. All the non-uniform N-bit binary string ($U > 2$) are grouped into a "miscellaneous" category. The mapping from LZP_N to LZP_N^{u2}, where superscript "u2" signifies the uniform patterns having at most U value of 2 and has total N * (N−1) + 3 distinct labels. It is implemented using a look-up table of 2^N distinct elements. It is observed that uniform representation of the LZP are more stable (less sensitive to noise) and the number of bins becomes significantly less, which makes matching computationally efficient.

3. Local directional ZigZag pattern

The LBP represents a non-directional first order circular derivative of local texture pattern which labels each pixel by thresholding a set of sampled point of its even space circular neighbourhood. It encodes the local micro-information as a binary string without considering the suitable neighboring relationship. Whereas LDP extracts the more detailed local textural information with the higher order directional derivative variation of each pixel neighborhood. However, this method marks only derivative directional neighbors to analyze local characteristic and loose the potential information between derivative directions. To make the descriptor more robust against noise and invariance to rotation, we propose local directional ZigZag pattern (LDZP) which incorporates directional edge information of a texture image. The LDZP descriptor is computed as follows: first the edge responses of the texture image is extracted using the Kirsch compass masks $\mathbb{G}$ shown in Eq. 4 in six different direction.

$$\mathbb{G}^0 = \begin{bmatrix} +5 & +5 & +5 \\ -3 & 0 & -3 \\ -3 & -3 & -3 \end{bmatrix} \tag{4}$$

The spatial coordinate of $P_n^{i,j}$ with respect to the origin of the Kirsch compass kernel, (x, y) and rotation with angle θ is given as,

$$\begin{aligned} x_i &= x_c + \cos(\theta) \times (i - x_c) - sin(\theta) \times (j - y_c) \\ y_j &= y_c + \sin(\theta) \times (i - x_c) + cos(\theta) \times (j - y_c) \end{aligned} \tag{5}$$

where (x_c, y_c) represents the spatial center coordinates of the kernel rotation and θ is the clockwise rotation angle having positive values of 0°, 30°, 60°, 90°, 120°, and 150° ($\theta \in [0°, 180°]$) with $i, j \in [1, 3]$. The directional edge response of a texture image I (Fig. 3(b)) in the direction of angle θ is computed by Eq. (6).

$$J_{(x,y)}^{\theta} = \int G^{\theta}(x,y) I(x,y) dxdy. \tag{6}$$

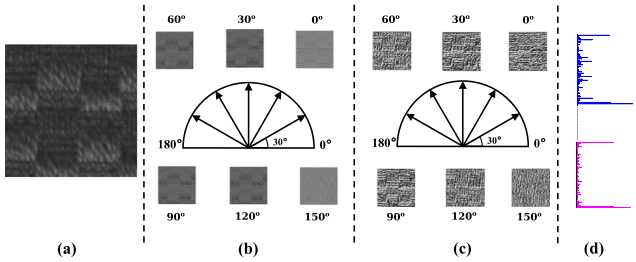

Fig. 3. (a) Texture sample. (b) Local directional edge maps. (c) $\text{LZP}_{N,\theta}^{u2}$ of the directional edge map J^{θ}. (d) local directional ZigZag pattern (LDZP) histogram.

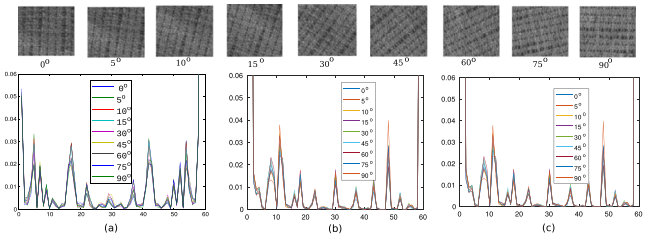

Fig. 4. The LDZP feature distribution for sample texture images of 9 different orientations taken from Outex_TC10 database: (a) without noise, (b) with noise corrupted by noise level of 10 dB SNR, (c) with noise corrupted by noise level of 30 dB SNR. Where abscissa and ordinate represent number of bins and feature probability distribution.

After identifying the local directional edge map (LDEM) $J^{\theta} \in \mathbb{R}^6$, $\text{LZP}_{N,\theta}^{u2}$ is computed for each θ from J^{θ} where $\theta \in \{0°, 30°, 60°, 90°, 120°, 150°\}$ (Fig. 3(c)). Finally LDZP is constructed by concatenating all the distribution of directional $\text{LZP}_{N,\theta}^{u2}$ i.e. $\{\text{LZP}_{N,\theta}^{u2}(J^{\theta}) | \theta = 0°, 30°, 60°, 90°, 120°, 150°\}$ (Fig. 3(d)). The LDZP descriptor overcomes the limitations of LBP features since LDZP is derived from the directional edge responses which are less sensitive to noise, and invariant to surface rotation. Fig. 4(a)–(c) show the examples of proposed LDZP feature distribution for the texture sample images taken from Outex_TC10 database (details in Section 6) having 9 different orientations (0°, 5°, 10°, 15°, 30°, 45°, 60°, 75°, and 90°) without noise, with noise corrupted by noise level of 10 dB SNR and 30 dB SNR, respectively. It is clearly observed that the LDZP feature distribution of different orientations are approximately overlapped for all cases which signifies LDZP descriptor is rotation invariant.

4. Local ZigZag pattern vs. local binary pattern

In conventional LBP, the neighboring sampling points that do not fall exactly within the integer pixel positions have been estimated by bi-linear interpolation or rounding operation which leads to the unreliable texture information due to inaccuracy of interpolation or rounding operation. In case of LBP the feature dimension exponentially increases with the number of sample points and it leads to difficulties in both computation and classification performance. However, the proposed LZP replaces the circular sampling structure of LBP by an effective ZigZag sampling structure (Fig. 2(a)) with respect to the center pixel. In this way all neighboring sampling points of the center pixel within a ZigZag sampling structure can fall exactly at the integer pixel positions and no bi-linear interpolation or rounding operation is needed. In addition, to avoid computational difficulties, we restrict the number of neighboring sample points to be a constant of 8 which encodes local texture information in atleast eight directions with respect to the center pixel that is sufficient to discriminate and provides reasonably good performance, whereas LBP with only 8 sample points is failed to achieve good performance (Table 2). Furthermore, in LBP,

Table 1
Summary of texture database used in experiment.

Texture Database	Image Rotation	Illumination Variation	Scale Variation	Texture Classes	Sample Size (pixels)	Samples per Class	Total Samples
Outex_TC10	✓			24	128 × 128	180	4320
Outex_TC12	✓	✓		24	128 × 128	200	4800

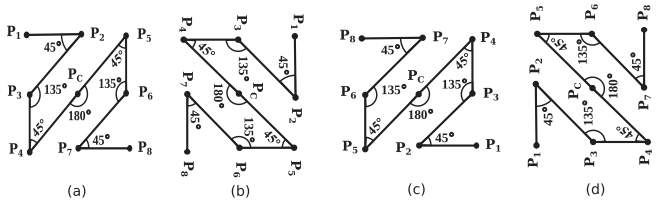

Fig. 5. (a)–(d) represent Local ZigZag structure (3 × 3) of four different orders for 8 neighboring with respect to center pixel and angular relationship among the neighbors.

the angular relation between any two consecutive sample point with respect to center is always to be a constant (45° for 8 sample points) and there is no visually perceptible angular relationship between two alternate pixel with respect to their intermediate. However, in Fig. 5, from second to the seventh pixel of the ZigZag scan, the two neighbors of each pixel extends angle either 45°, 180° or 135°. In Fig. 5(a), the formed angles $\measuredangle P_1P_2P_3$, $\measuredangle P_2P_3P_4$, $\measuredangle P_3P_4P_5$, $\measuredangle P_4P_5P_6$, $\measuredangle P_5P_6P_7$, $\measuredangle P_6P_7P_8$, and $\measuredangle P_7P_8P_9$ are 45°, 135°, 45°, 180°, 45°, 135°, 45° respectively and preserved a spatial cohesion between neighbouring pixels. Also in case of Lzp the angle extended at the reference pixel by two consecutive pixels in ZigZag scan varies while in case of Lbp this angle is constant and equal to 45°. These angular variations of Lzp among the sample points capture more frequent changes in local texture pattern. Such structure makes Lzp better texture descriptor than traditional Lbp based descriptors. Also, computation of the Lzp is more efficient than Lbp for the same feature size. In addition, the classification performances of Lzps are nearly equal (Fig. 9) over different order of Local ZigZag structures of Fig. 5(a)-(d).

5. Similarity matching using Ldzp

In this work, the texture classification is performed via non-parametric Nnc classifier. The Nnc with χ^2-distance [4,7,20] is used to show the effectiveness of the proposed Ldzp descriptor. Two histograms $H_1 = u_1, \ldots, u_M$ and $H_2 = w_1, \ldots, w_M$, are compared using χ^2 distance, defined as follows, $D(H_1, H_2) = \sum_{i=1}^{M} \frac{(u_i - w_i)^2}{u_i + w_i}$, where M represents the total number of bins, H_1 and H_2 represent the extracted features of a trained model and test sample. The class of test sample H_1 is assigned to the class of trained model H_2 for which the χ^2-distance is minimized.

6. Results and discussion

To figure out the texture classification performance of the proposed Ldzp descriptor, experiments are carried out on two large and commonly used well-known Outex_TC_00010 (TC10) and Outex_TC_00012 (TC12) [28] texture databases. These databases contain 24 classes of homogeneous texture images of size 128 × 128 pixels. **Outex_TC_00010 (Outex_TC10)** contains texture images under illuminant "inca" whereas **Outex_TC_00012 (Outex_TC12)** contain texture images with 3 different illuminants ("inca", "horizon", and "t184"). Both of Outex test suits images are collected under 9 different rotation angels (0°, 5°, 10°, 15°, 30°, 45°, 60°, 75°, and 90°) in each texture class. The experimental test suites **Outex_TC10**, and **Outex_TC12** are summarized in Table 1. Some example images of the Outex database are shown in Fig. 6.

Table 2
Average classification accuracy (%) of Ldzp descriptor and state-of-the-art schemes on Outex_TC10 and Outex_TC12.

Method	Classifier	Outex_TC10	Outex_TC12		Average
			horizon	t184	
Ltp [24]	Nnc	76.06	63.42	62.56	67.34
Var [16]	Nnc	90.00	64.35	62.93	72.42
Lbp [4]	Svm	97.60	85.30	91.30	91.40
$\text{Lbp}^{riu2}_{R,N}$	Nnc	84.89	63.75	65.30	71.31
LBP/VAR	Nnc	96.56	78.08	79.31	84.65
$\text{Lbpv}^{riu2}_{R,N}$ [19]	Nnc	91.56	77.01	76.62	81.73
CLBP_S	Nnc	84.81	63.68	65.46	71.31
CLBP_M	Nnc	81.74	62.77	59.30	67.93
CLBP_M/C	Nnc	90.36	76.66	72.38	79.80
CLBP_S_M/C [20]	Nnc	94.53	82.52	81.87	86.30
CLBP_S/M	Nnc	94.66	83.14	82.75	86.85
CLBP_S/M/C	Nnc	98.93	92.29	90.30	93.05
$\text{Lbp}^{NT}_{R,N}$ [30]	Nnc	99.24	96.18	94.28	96.56
$\text{Dlbp}_{R=3,N=24}$ [18]	Svm	98.10	87.40	91.60	92.36
Brint [25]	Nnc	99.35	97.69	98.56	98.53
VZ-MR8 [5]	Nsc	93.59	92.82	92.55	92.99
VZ-Patch [7]	Nsc	92.00	92.06	91.41	91.82
Ptp [29]	Nnc	99.56	98.08	97.94	98.52
Lddp [23]	Nnc	97.89	93.40	95.30	95.53
Drlbp [31]	Nnc	99.19	95.80	96.72	97.23
Cdcp [26]	Nnc	99.76	99.82	99.62	99.72
Proposed Ldzp	Nnc	**99.95**	**99.93**	**99.82**	**99.90**

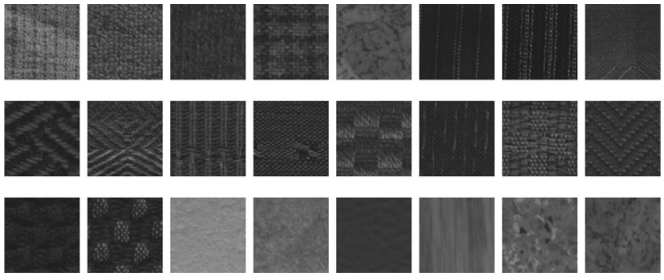

Fig. 6. Random samples of 24 texture images in Outex_TC10 and Outex_TC12 texture suits.

The performance of Ldzp descriptor are evaluated in term of classification accuracy using K-fold cross-validation test along with non-parametric nearest neighbor classifier (Nnc) with Chi-Squre (χ^2) distance. In K-fold cross-validation test, the feature set of each category is randomly sorted and divided into K-folds ($K = 10$), where $K - 1$ folds is used to train the classifier and remaining one fold has been used to test the performance. Average of the classification accuracies over K rounds get a final cross-validation accuracy. The K-fold cross-validation process provides a more reliable picture of the classification performance. The performance of the proposed descriptor is compared with $\text{Lbp}^{riu2}_{R,N}$ [4], Dlbp [18], multi-scale $\text{Clbp\_S}^{riu2}_{R,N}/\text{M}^{riu2}_{R,N}/\text{C}(1, 8+3, 16+5, 24)$ [20], $\text{Lddp}^{riu2}_{R,N}$ [23], Ltp [24], Ptp [29], Brint [25], $\text{Lbp}^{NT}_{R,N}$ [30], VZ-MR8 [5], VZ-Patch [7] and other state-of-the-art methods.

The comparative results of the classification accuracy (%) are tabulated in Table 2. We have made the following observations from the results of the experiment. The classification rate

of locally rotation invariant $\text{LBP}^{riu2}_{R,N}/\text{VAR}_{R,N}$ is better than $\text{LBP}^{riu2}_{R,N}$ as $\text{LBP}^{riu2}_{R,N}/\text{VAR}_{R,N}$ computed the joint distribution of LBP and local variance of a texture image, which are complementary. CLBP_$S^{riu2}_{R,N}/M^{riu2}_{R,N}/C(1{,}8 + 2{,}16 + 3, 24)$ which is made by fusing the CLBP_S and CLBP_M/C, provides better performance compared to the other variant of CLBP. This is because it contains complementary features of sign and magnitude, in addition to the center pixel which represents the gray level of the local patch. The DLBP + NGF [18], makes use of the most frequently occurred patterns (around 80%) of LBP to improve the recognition rate compared to original $\text{LBP}^{u2}_{R,N}$. However, it neglects the local spatial structure, which is important for texture discrimination and needs pre training stage for dimensionality selections. The MR8 is a state-of-the-art texton based statistical algorithm, where the VZ-MR8 and VZ-Patch takes dense response from multiple filters. However, the performance is significantly low compared to the proposed LDZP. In addition, feature extraction and matching complexity are quite high [7] because the MR8 needs to find 8 maximum responses after 38 filters are convolving with the image and compares every 8-dimension vector in an image with all the textons to build histograms using clustering technique. $\text{LBP}^{NT}_{R,N}$ [30] based methods and BRINT [25] give better performance compared to other state-of-the-art LBP methods. However, the accuracies are lower than those obtained by our proposed LDZP. This is mainly because $\text{LBP}^{NT}_{R,N}$ extracts features by using locally rotation invariant $\text{LBP}^{riu2}_{R,N}$ approach which produces only 10 bins and such small size of features can not represent each class well, while BRINT method extracted large number of features from multiple resolution ($R = 1, 2, 3, 4$) by utilizing rotation invariant $\text{LBP}^{ri}_{R,N}$ approach, whereas it loses the global image information.

Finally, result table shows the proposed LDZP descriptor achieves state-of-the-art performance in term of mean accuracy and standard deviations 99.95 ± 0.119%, 99.93 ± 0.156%, and 99.82 ± 0.196% on three different test suits Outex_TC10, and Outex_TC12 (“horizon”, and “t184”), respectively. It can also be observed that the superiority of the proposed LDZP descriptor over state-of-the-art classification methods on both Outex_TC10 which contains texture under different illumination and Outex_TC12 contains texture under rotation variations along with different illumination situations. The proposed descriptor provides superior performance because it has following attributes: The proposed LZP replaces the circular sampling structure of LBP by an effective ZigZag sampling structure with respect to the center pixel. In this way all neighbors of the center pixel within a ZigZag sampling structure can fall exactly at the integer pixel positions which avoids the unreliable texture information due to inaccurate bi-linear interpolations of gray intensities; LZP provides a strong varying angular relation between two consecutive pixels with respect to the center as well as two alternate pixel with respect to their intermediate which effectively encodes more frequent changes in local texture pattern; To compute the LDZP descriptor we calculate local directional edge map (LDEM) of a texture image using the Kirsch compass mask in six different directions and encodes all directional edge responses using LZP and which makes the descriptor rotation invariant. Fig. 7 shows the confusion matrix for classification performance of proposed LDZP on Outex_TC10 and Outex_TC12 databases.

In addition, the individual classification accuracy of proposed LDZP against six different angles (0°, 30°, 60°, 90°, 120° and 150°) of Kirsch compass masks are evaluated on Outex_TC10 and Outex_TC12 databases. Fig. 8 shows the mean classification accuracy of the proposed LDZP descriptors, extracted from the edge responses of a texture image with six different angles of Kirsch compass masks (0°, 30°, 60°, 90°, 120° and 150°) (Fig. 3 (b)) for Outex_TC10 and Outex_TC12 (“horizon” and “t184”) databases. The average classification performances of the proposed LDZP on Outex databases for four different ZigZag orders (Fig. 5(a)–(d)) are shown in Fig. 9. It is observed that the performances of proposed LDZP are approximately equal over selection of different order of Local ZigZag structures.

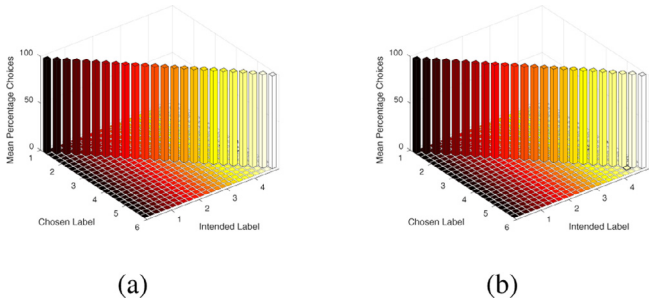

Fig. 7. Confusion matrix (in sorted) for classification performance of proposed LDZP on (a) Outex_TC10 and (b) Outex_TC12 databases.

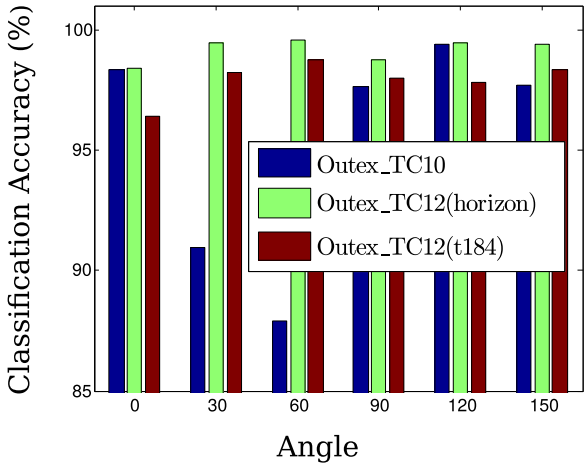

Fig. 8. The classification accuracy against six different angles (0°, 30°, 60°, 90°, 120° and 150°) of Kirsch compass masks for Outex database.

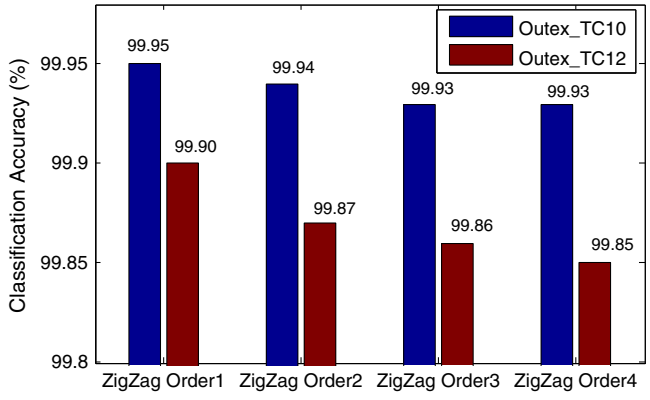

Fig. 9. The average classification accuracy of proposed LDZP on Outex databases for four different ZigZag orders (Fig. 5(a)–(d)).

Though the trend is clear from the performance Table 2, we have further analysed the performance using one way statistical analysis of variance (ANOVA) test [32]. The null hypothesis H_0 for the test indicates that, *there is no significant difference among group means*. We can reject H_0 if the p-value for an experiment is less than the selected significant level, which implies that the at least one group mean is significantly different from the others. To understand the performance of the proposed descriptor LDZP was significantly differs than well-known descriptors such as PTP, BRINT, VZ-MR8, and CLBP_S/M/C, we conduct an one way ANOVA test with

Table 3
One way statistical ANOVA test result for Outex_TC10 & Outex_TC12 (horizon and t184) texture databases, where level of significance selected as $\alpha = 0.05$.

Source	SS	df	MS	F	Prob (p) > F
Groups	116.669	04	29.1674	6.57	**0.0074**
Error	044.425	10	04.4425		
Total	161.094	14			

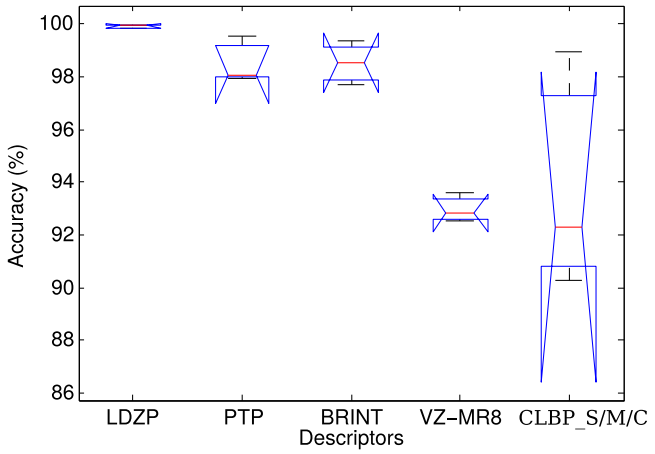

Fig. 10. The box plot (descriptor vs. accuracy) corresponding to one way statistical ANOVA test for proposed LDZP and other state-of-the-art methods on Outex_TC10 & Outex_TC12 (horizon and t184) texture databases.

significance level is kept as $\alpha = 0.05$ and the test results are shown in Table 3. It is observed from Table 3, the p-value (0.0074) is less than the selected significant level $\alpha = 0.05$, which indicates the performance of proposed descriptor significantly differs from other descriptors and hence reject the hypothesis H_0. In addition, the box plot corresponding to aforementioned ANOVA test is shown in Fig. 10, which clearly indicates the mean performance of proposed descriptor significantly better than the well-known descriptors such as PTP [30], BRINT [25], VZ-MR8 [5], VZ-Patch [7] and CLBP_S/M/C [20].

To visualize the texture classification performance of the proposed descriptor in term of Receiver Operating Characteristics (ROC) and Area Under Curve (AUC) [33], the experiments were carried out with K-folds cross validations ($K = 10$) test in slightly different way than before. Here one fold is used to train the NNC classifier while remaining $K - 1$ folds have been used to test the performance of proposed descriptor. Though the number of training samples is very less compared to test samples, the proposed descriptor achieves average classification accuracy and standard deviation of 95.10 ± 0.6303%, 94.68 ± 1.1299% and 92.35 ± 1.2251% for Outex_TC10 and Outex_TC12 (horizon & t184) test suits, respectively. The ROC plot with AUC of the proposed descriptor corresponding to above mentioned experiment is depicted in Fig. 11. It is observed from Fig. 11 that the proposed descriptor achieves AUC values of 95.06%, 93.63% and 93.04%, respectively for Outex test suits.

In addition, Table 4 demonstrates the noise robustness of different methods on Outex_TC10 database by comparing the classification rates for different noise levels (measured using SNR i.e Signal to Noise Ratio). The proposed descriptor achieves state-of-the-art results in term of mean accuracy and standard deviations 99.91 ± 0.1195%, 99.91 ± 0.1195%, 99.90 ± 0.1619%, 99.88 ± 0.1637%, and 99.88 ± 0.2250% on SNR = 100 dB, 30 dB, 15 dB, 10 dB, and 5 dB, respectively. It is observed that the change of standard deviations with the SNR levels shows the LDZP descriptor is more robust to noise compared to other state-of-the-art methods. When SNR

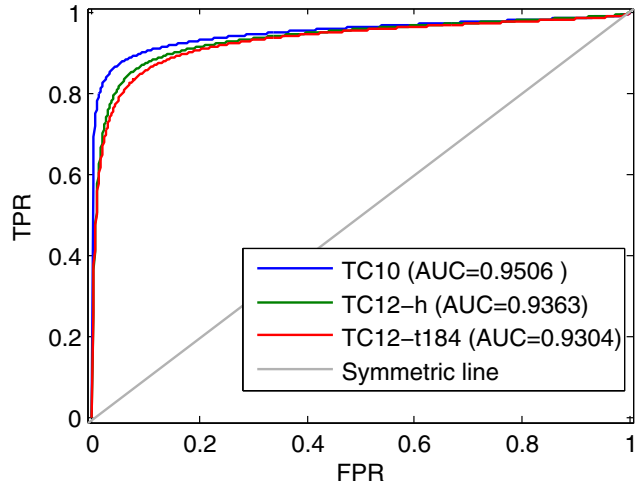

Fig. 11. The area under the ROC curve (AUC) corresponds to the probability that a model outputting a score between 0 and 1 ranks a randomly chosen positive sample higher than a randomly chosen negative sample.

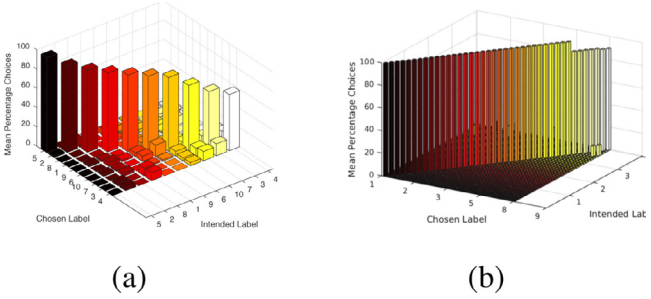

Fig. 12. Confusion matrix (in sorted) for classification performance of proposed LDZP on (a) Yale B and (b) ORL face databases.

decreases, the classification accuracy is nearly constant whereas it drops for other state-of-the-art methods.

To study the effectiveness of the proposed LDZP descriptor for other images like human face, the experiments are carried on Yale B [36] and ORL [37] face databases using K-folds ($K = 10$) cross validation test. Yale B database consists of 5760 face images of ten individuals. The images are taken under 9 different pose and 64 different illumination conditions. ORL database consists of images taken from 40 different individuals with 10 images of each person. The images were taken at different times, varying the lighting, facial expressions (open/closed eyes, smiling/not smiling) and facial details (glasses/no glasses). All the images were taken against a dark homogeneous background with the subjects in an upright, frontal position (with a tolerance for some side movement) [38]. The comparative performances of face recognition using proposed descriptor and other state-of-the-art descriptors like LTrP [39], LVP [40], LTP [24], LBP [4] are tabulated in Table 5. Experimental results indicate that the proposed descriptor achieves average recognition performances of 77.33% and 98.25% for Yale B and ORL databases, respectively. Experimental results in Table 5 also indicate that proposed LDZP descriptor effectively work on face images and provide better or comparative recognition performances compared to other state-of-the-art descriptors. Fig. 12 shows the Confusion matrix for classification performance of the proposed LDZP on Yale B and ORL face databases.

We have implemented the algorithm in MATLAB 2011 environment and executed the program on Intel® Core™2 Duo CPU T6400 @ 2.00 GHz × 2 processor and 3GB RAM with UBUNTU 14.04 LTS operating system. The average feature extraction and matching

Table 4
Classification accuracy (%) of proposed method and different state-of-the-art methods on Outex_TC10 with different noise levels in term of dB.

Methods	Classifier	Classification Accuracy (%)				
		SNR = 100	SNR = 30	SNR = 15	SNR = 10	SNR = 5
$LBP^{NT}_{R,N,k}$ [30]	NNC	–	99.79	99.76	99.76	99.74
$LTP^{riu2}_{R=3,N=24}$ [34]	NNC	99.45	98.31	93.44	84.32	57.37
$NRLBP^{riu2}_{R,N}$ [35]	NNC	84.49	81.16	77.52	70.16	50.88
BRINT [25]	NNC	97.76	96.48	95.47	92.97	88.31
Proposed LDZP	NNC	**99.91**	**99.91**	**99.90**	**99.88**	**99.88**

Table 5
The comparative results for face recognition performances of proposed descriptor and other state-of-the-art descriptors using 10-folds cross validation test.

Face Data	Method	Round-1	Round-2	Round-3	Round-4	Round-5	Round-6	Round-7	Round-8	Round-9	Round-10	Average
Yale B [36]	LTrP [39]	70.83	68.57	70.00	70.00	71.42	66.67	63.33	80.00	80.00	68.33	70.83
	LVP [40]	81.42	62.85	74.28	81.42	81.42	75.00	76.67	75.00	81.67	83.33	77.30
	LTP [24]	38.57	47.14	37.14	44.28	45.71	50.00	36.67	36.67	40.00	41.67	41.78
	LBP [4]	31.42	52.85	48.57	45.71	40.00	35.00	43.33	35.00	48.33	41.66	42.19
	LDZP	77.14	74.28	84.28	81.42	72.85	76.67	73.33	76.67	75.00	81.67	**77.33**
ORL [37]	LTrP [39]	97.50	100.00	100.00	97.00	95.00	95.00	92.00	95.00	95.00	100.00	96.75
	LVP [40]	100.00	100.00	95.00	97.50	97.50	97.00	97.00	97.50	97.00	100.00	98.00
	LTP [24]	95.00	92.50	92.50	100.00	97.50	97.50	95.00	97.50	97.50	92.80	95.75
	LBP [4]	90.00	100.00	87.00	92.50	97.50	92.50	92.50	97.50	95.00	95.00	94.25
	LDZP	100.00	95.00	97.50	100.00	100.00	97.00	95.00	100.00	97.80	100.00	**98.25**

time (in seconds) cost per-image by the proposed LDZP descriptor on two benchmark texture databases take 0.20 s and 0.27 s for both Outex_TC10 and Outex_TC12 ("horizon" and "t184"). It has been observed that the matching complexity of the LDZP descriptor varies linearly with number of training samples. It shows that the proposed LDZP descriptor is fast enough for real time scenario.

7. Conclusion

In this letter, we proposed a novel and efficient descriptor for rotation invariant texture image classification by exploring the local directional ZigZag pattern (LDZP). To compute LDZP descriptor, at first directional edge response of a texture image is obtained using Kirsch compass mask in six different directions. Then the proposed local ZigZag pattern (LZP) which characterize local spatial ZigZag structure of texture is used to encode directional edge responses. Finally, LDZP feature descriptor is obtained by concatenating uniform pattern histograms of directional LZP map. The proposed descriptor is highly discriminative, robust on illumination changes and texture rotation, and also less sensitive to noise with advantages of computational simplicity. Experimental results on two Outex test suits for texture classification shows performance of the proposed LDZP descriptor provides superior texture classification performance compared to state-of-the-art methods and effectively work as face image descriptor also.

Acknowledgements

The authors would like to thank Machine Vision Group, University of Oulu, Finland and Visual Geometry Group, University of Oxford, UK for sharing the program codes of LBP and VZ_MR8.

References

[1] M. Tuceryan, A.K. Jain, et al., Texture analysis, Handbook Pattern Recognit. Comput. Vis. 2 (1993) 207–248.
[2] R.M. Haralick, K. Shanmugam, et al., Textural features for image classification, IEEE Trans. Syst. Man Cybern. (6) (1973) 610–621.
[3] T. Randen, J.H. Husoy, Filtering for texture classification: a comparative study, IEEE Trans. Pattern Anal. Mach. Intell. 21 (4) (1999) 291–310.
[4] T. Ojala, M. Pietikainen, T. Maenpaa, Multiresolution gray-scale and rotation invariant texture classification with local binary patterns, IEEE Trans. Pattern Anal. Mach. Intell. 24 (7) (2002) 971–987.
[5] M. Varma, A. Zisserman, A statistical approach to texture classification from single images, Int. J. Comput. Vis. 62 (1–2) (2005) 61–81.
[6] J. Zhang, M. Marszałek, S. Lazebnik, C. Schmid, Local features and kernels for classification of texture and object categories: a comprehensive study, Int. J. Comput. Vis. 73 (2) (2007) 213–238.
[7] M. Varma, A. Zisserman, A statistical approach to material classification using image patch exemplars, IEEE Trans. Pattern Anal. Mach. Intell. 31 (11) (2009) 2032–2047.
[8] M. Crosier, L.D. Griffin, Using basic image features for texture classification, Int. J. Comput. Vis. 88 (3) (2010) 447–460.
[9] L. Liu, P. Fieguth, Texture classification from random features, IEEE Trans. Pattern Anal. Mach. Intell. 34 (3) (2012) 574–586.
[10] J. Zhang, T. Tan, Brief review of invariant texture analysis methods, Pattern Recognit. 35 (3) (2002) 735–747.
[11] I. WEISS, Geometric invariants and object recognition, Int. J. Comput. Vis. 10 (3) (1993) 207–231.
[12] R.L. Kashyap, A. Khotanzad, A model-based method for rotation invariant texture classification, IEEE Trans. Pattern Anal. Mach. Intell. (4) (1986) 472–481.
[13] J. Mao, A.K. Jain, Texture classification and segmentation using multiresolution simultaneous autoregressive models, Pattern Recognit. 25 (2) (1992) 173–188.
[14] J.-L. Chen, A. Kundu, Rotation and gray scale transform invariant texture identification using wavelet decomposition and hidden Markov model, IEEE Trans. Pattern Anal. Mach. Intell. 16 (2) (1994) 208–214.
[15] H. Deng, D.A. Clausi, Gaussian MRF rotation-invariant features for image classification, IEEE Trans Pattern Anal Mach Intell 26 (7) (2004) 951–955.
[16] T. Ojala, M. Pietikäinen, D. Harwood, A comparative study of texture measures with classification based on featured distributions, Pattern Recognit 29 (1) (1996) 51–59.
[17] P. Matti, H. Abdenour, Z. Guoying, et al., Computer vision using local binary patterns, 2011,
[18] S. Liao, M.W. Law, A.C. Chung, Dominant local binary patterns for texture classification, IEEE Trans. Image Process. 18 (5) (2009) 1107–1118.
[19] Z. Guo, L. Zhang, D. Zhang, Rotation invariant texture classification using lbp variance (lbpv) with global matching, Pattern Recognit. 43 (3) (2010) 706–719.
[20] Z. Guo, L. Zhang, D. Zhang, A completed modeling of local binary pattern operator for texture classification, IEEE Trans. Image Process. 19 (6) (2010) 1657–1663.
[21] B. Zhang, Y. Gao, S. Zhao, J. Liu, Local derivative pattern versus local binary pattern: face recognition with high-order local pattern descriptor, IEEE Trans. Image Process. 19 (2) (2010) 533–544.
[22] S.R. Dubey, S.K. Singh, R.K. Singh, Local wavelet pattern: a new feature descriptor for image retrieval in medical ct databases, IEEE Trans. Image Process. 24 (12) (2015) 5892–5903.
[23] Z. Guo, Q. Li, J. You, D. Zhang, W. Liu, Local directional derivative pattern for rotation invariant texture classification, Neural Comput. Appl. 21 (8) (2012) 1893–1904.
[24] X. Tan, B. Triggs, Enhanced local texture feature sets for face recognition under difficult lighting conditions, IEEE Trans. Image Process. 19 (6) (2010) 1635–1650.
[25] L. Liu, Y. Long, P.W. Fieguth, S. Lao, G. Zhao, Brint: binary rotation invariant and noise tolerant texture classification, IEEE Trans. Image Process. 23 (7) (2014) 3071–3084.

[26] S.K. Roy, B. Chanda, B.B. Chaudhuri, D.K. Ghosh, S.R. Dubey, A complete dual-cross pattern for unconstrained texture classification, in: 4th Asian Conference on Pattern Recognition (ACPR 2017), Nanjing, China, 2017, pp. 741–746.
[27] D. Salomon, Data Compression: the Complete Reference, Springer Science & Business Media, 1998.
[28] T. Ojala, T. Maenpaa, M. Pietikainen, J. Viertola, J. Kyllonen, S. Huovinen, Outex-new framework for empirical evaluation of texture analysis algorithms, in: Pattern Recognition, 2002. Proceedings. 16th International Conference on, 1, IEEE, 2002, pp. 701–706.
[29] K. Wang, C.-E. Bichot, C. Zhu, B. Li, Pixel to patch sampling structure and local neighboring intensity relationship patterns for texture classification, IEEE Signal Process. Lett. 20 (9) (2013) 853–856.
[30] A. Fathi, A.R. Naghsh-Nilchi, Noise tolerant local binary pattern operator for efficient texture analysis, Pattern Recognit. Lett. 33 (9) (2012) 1093–1100.
[31] R. Mehta, K. Egiazarian, Dominant rotated local binary patterns (drlbp) for texture classification, Pattern Recognit. Lett. 71 (2016) 16–22.
[32] F. Anscombe, The validity of comparative experiments, J. R. Stat. Soc. Ser. A 111 (3) (1948) 181–211.
[33] T. Fawcett, An introduction to roc analysis, Pattern Recognit. Lett. 27 (8) (2006) 861–874.
[34] X. Tan, B. Triggs, Enhanced local texture feature sets for face recognition under difficult lighting conditions, in: International Workshop on Analysis and Modeling of Faces and Gestures, Springer, 2007, pp. 168–182.
[35] J. Ren, X. Jiang, J. Yuan, Noise-resistant local binary pattern with an embedded error-correction mechanism, IEEE Trans. Image Process. 22 (10) (2013) 4049–4060.
[36] A.S. Georghiades, P.N. Belhumeur, D.J. Kriegman, From few to many: illumination cone models for face recognition under variable lighting and pose, IEEE Trans. Pattern Anal. Mach. Intell. 23 (6) (2001) 643–660.
[37] F.S. Samaria, A.C. Harter, Parameterisation of a stochastic model for human face identification, in: Applications of Computer Vision, 1994., Proceedings of the Second IEEE Workshop on, IEEE, 1994, pp. 138–142.
[38] R. Mehta, J. Yuan, K. Egiazarian, Face recognition using scale-adaptive directional and textural features, Pattern Recognit. 47 (5) (2014) 1846–1858.
[39] S. Murala, R. Maheshwari, R. Balasubramanian, Local tetra patterns: a new feature descriptor for content-based image retrieval, IEEE Trans. Image Process. 21 (5) (2012) 2874–2886.
[40] K.-C. Fan, T.-Y. Hung, A novel local pattern descriptorlocal vector pattern in high-order derivative space for face recognition, IEEE Trans. Image Process. 23 (7) (2014) 2877–2891.